Research Article

Piotr Bogacz*

Degradation of flood embankments – Results of observation of the destruction mechanism and comparison with a numerical model

https://doi.org/10.1515/eng-2017-0031
Received June 22, 2017; accepted Sep 27, 2017

Abstract: The paper presents the results of model tests conducted for a flood embankment under varying conditions of saturation. Test embankments were formed from the natural sea sand. The test apparatus consisted of the box with internal dimensions 200 × 100 × 4.5 cm , and thus ensured the implementation of the plane strain state. In most tests during watering air entrapment was observed, leading to formation of open soil discontinuities, called macropores (their dimensions many times exceeded the grain size of the soil skeleton). Analysis of images from a number of tests allowed to create a simplified model of the evolution of a macropore. The numerical model has been based on the finite element method using the PLAXIS 2D software. A comparison has been made between the observation of the phenomena occurring in the physical model and the results of the simulation of the phenomena in the numerical model. A correlation has been proven between the results acquired in reality and the results derived from the numerical model.

Keywords: flood embankment, variable saturation conditions, finite elements method analysis

1 Introduction

A flood embankment, an artificial escarpment-shaped fill, whose primary parameter is its width, constitutes an important element for the protection of people, animals and property against water surges. During its operation, the flood embankment is repeatedly subjected to the impact of destructive factors, the most important of which seems to be the variable saturation level. It increases during heavy or long-lasting atmospheric precipitation as well as spring melting, and decreases during dry periods. This is not without significance for the stability of flood embankment construction.

There are not many papers dealing with the phenomenon of closing air in the pores of the ground. [13] proposed a conceptual model of soil containing large gas bubbles. The number of papers on the topic is limited, probably due to the complexity of these phenomena and the difficulty in testing them by experimental methods [1, 5, 11–18]. An important work on the appearance of open discontinuities is Shin and Santamarina [10], which describes the different types of cracks caused by water or gas. With a small amount of papers, it is not possible to create reliable theoretical models and their implementation in numerical methods.

The behavioural observations of the flood embankment models were conducted in the years 2006-2013 in the Institute of Hydroengineering of the Polish Academy of Sciences in Gdańsk. The grants on which the research was conducted are given in references.

2 Methodology

The starting point for the model tests was the experiments conducted by Maghdy Abo Elela [1], who, during simulations of rain, observed the entrapment of air in the central zone of the body of the flood embankment model, as well as an escape route for air from this area.

The experiments described in this paper were conducted in a test rig constructed and tested in IBW PAN (Institute of Hydroengineering Polish Academy of Sciences), used in 1996 by Abo Elela. In 2006, this test rig was modernised by adding a system of sensors to measure the pressure of air and water in soil pores. In 2011 other changes were introduced, facilitating the acquisition of a more complete record and digital analysis [2, 8, 9].

The test rig (Figure 1) for researching the flood embankment model, consisted of a box with internal dimen-

*Corresponding Author: Piotr Bogacz: Uniwersytet Warmińsko-Mazurski w Olsztynie, Wydział Geodezji, Inżynierii Przestrzennej i Budownictwa, Instytut Budownictwa, 10-724 Olsztyn, ul. Jana Heweliusza 4; Email: piotr.bogacz@uwm.edu.pl

sions of 200 × 100 × 4.5 cm which thus enabled the construction of the so-called slit model, meaning a model whose one dimension (the depth in a direction perpendicular to the cross-section) is considerably smaller than the remaining two dimensions. This configuration ensured the conditions of a plane strain state.

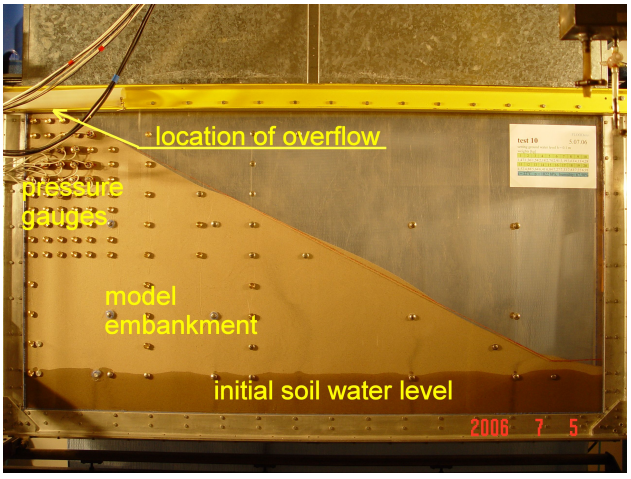

Figure 1: Components of the test rig.

The geometry of a model corresponding to the landward or riverward (Figure 2a) part of the flood embankment was used in the first part of the research (type 1). One advantage of such a shape of the model was the ability to increase its height to 1 m; its disadvantage being the introduction of an impermeable border inside the body – which did not correspond to the factual working conditions of the most frequently observed flood embankment types. The second part of the research (type 2) was conducted on a full flood embankment model (Figure 2b) with the slopes inclined in a similar manner to the slope from the first model. One disadvantage of this model, resulting from the limitations of the measurement box, was the height, which equalled 0.5 m. A substrate with a height of 0.4 m was used in order to increase it. In all cases, the model was formed using the sand rain method [7]. Lubiatowo-type sand, whose characteristics are presented in Table 1, was used in the construction of the type 1 model. The same sand was used to build a substrate in the type 2 model. The body of the type 2 model was built of quartz sand, the characteristics of which are also presented in Table 1.

The programme of the modelling studies, involved three methods of saturating the model, all of them simulating intense rain – landward slope, water flowing over the top of the flood embankment, as well as a change in the water level from the riverward slope side [2].

Table 1: Characteristics of the Lubiatowo and quartz sand used to the tests.

Variable	Value - Lubiatowo sand	Value – quartz sand
Median d_{50}	0.25 mm	0.125 mm
Filtration coefficient k_s	0.016 cm/s	0.009 cm/s
Bulk density	17.0 kN/m^3	15.6 kN/m^3

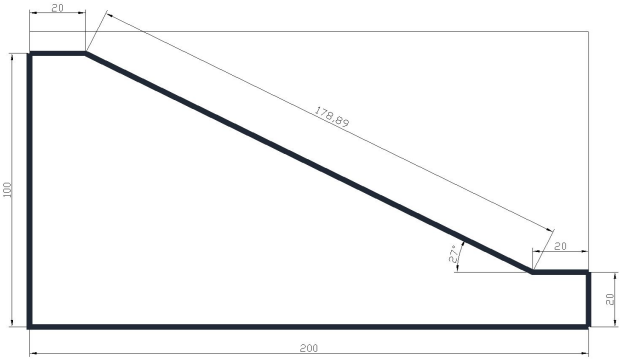

Figure 2a Geometry adopted for the examination of one of the flood embankment model's slopes.

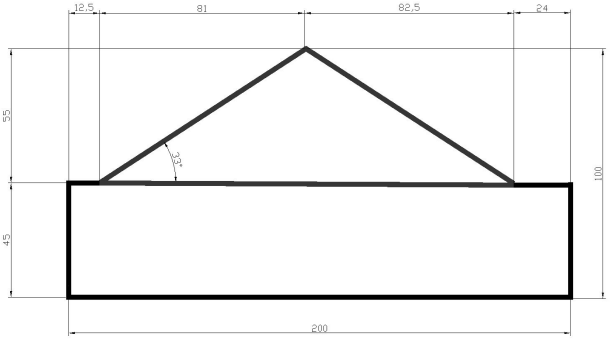

Figure 2b Geometry adopted for the examination of a complete model of the flood embankment.

The boundary condition for the F10 and F14 tests (type 1) - ground water level was set at h = 10cm from the bottom of the model. Type 2 tests did not set ground water level. The tests were performed on a dry model.

3 Results of the observation of the physical model

The initial observation results were described earlier [2, 4, 6]. In most tests, during saturation of the flood embankment model, a phenomenon was observed involving the entrapment of air in areas which remained dry for a cer-

tain time period, in spite of being surrounded from the outside by saturated soil. As a result of the further evolution of these areas, there were instances of the appearance of open discontinuities, which took the form of variously shaped fissures filled with air. They have been described as macropores, since their dimensions correspond to a much higher number (about several thousand) of soil grains compared to what was assumed by [12] when defining "large gas bubbles" (20-30 grains). A general image of a macropore is presented in Figure 3.

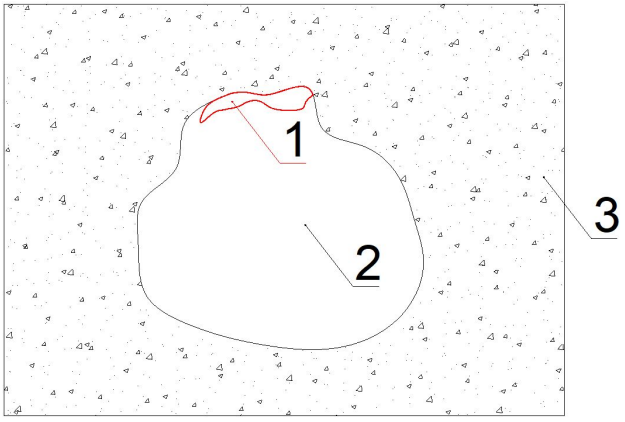

Figure 3: General image of a macropore: 1 – an open macropore filled with air, 2 – dry soil – supply area of the macropore, 3 – saturated soil.

For most of its existence, a typical macropore (some are very stable and do not dissipate until the end of the experiment) is created at the upper edge of the air entrapment area, although on the dry soil side. When saturating the model, the macropore volume increases at the expense of shrinking the supply area, and the water from which pushes the air confined in the soil pores upward. The supply area (air entrapment area) keeps shrinking after losing contact with air from the atmosphere, which must result in the compression of air within the continuously decreasing volume. Upon exceeding the threshold value of pressure, the air is released from the soil pores and creates a macropore, the volume of which initially increases and then stabilises. The pressure in a macropore which is stabilised with respect to volume must keep increasing, because upon reaching another threshold value (or reduction of the weight of soil above the macropore due to micro-sliding) the air is rapidly released into the atmosphere. The release of air leads either to dissipation of the macropore along with the supply area, or to an extreme decrease in its volume. Usually, after the escape of air, the soil structure remains disturbed with visible subtle, closed fractures – the relics of macropores.

The collective location of the created macropores for selected tests during model-based studies is presented in Figure 4.

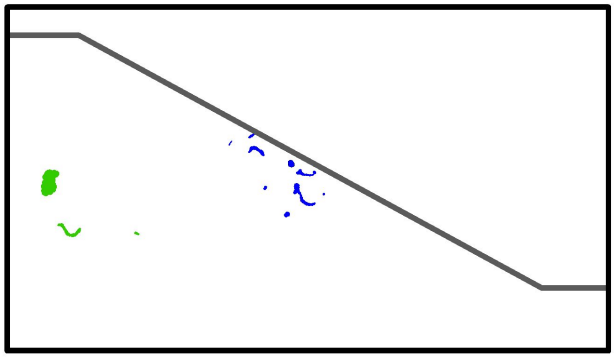

Figure 4: Location of the largest macropores in a cross-section of the model (type 1): red colour – test F10, green colour – test F15.

In all tests (except for the type 2 model test), regardless of the method of saturation, progressive destruction of the model slope occurred following a similar sequence (Figure 5 – 6). The destruction process started at the foot of the embankment and involved the sliding of small separated lumps along a relatively flat slide plane, extending at a depth of approximately 18.5 cm, as measured from the inclined profile of the embankment. A single destruction episode involving the sliding of an individual lump has been described as a "micro-slide". The range of subsequent micro-slides is shown in Figures 5 – 6 as a black dashed line. A solid black line corresponds to the initial

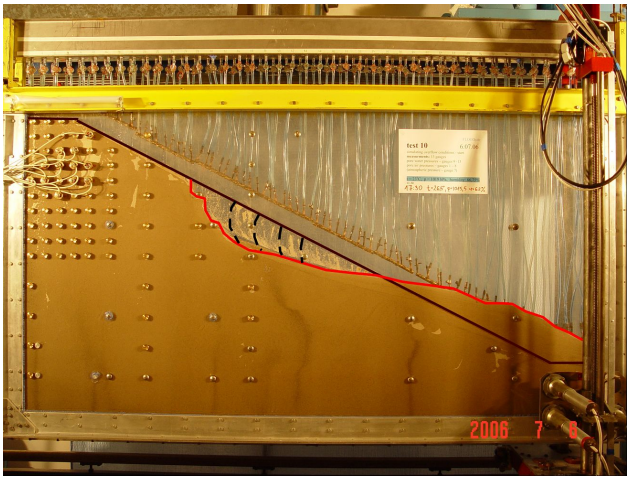

Figure 5: Embankment destruction mechanism (type 1 model) - test F10 - test using a rain generator with a water outlet of qi ~ 10 ml/s.

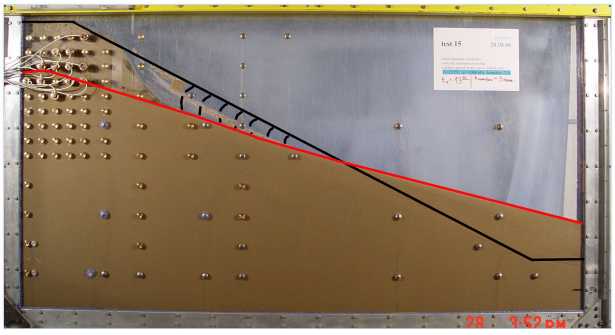

Figure 6: Embankment destruction mechanism (type 1 model) - test F15 - a test with water overflow through the crown of the flood embankment about q ~ 4 ml/s.

profile of the embankment, with the final one represented by the red line.

Mechanism of destruction of model type 2 (Figure 2b) is shown in Figure 7. As the water Table is raised, it infiltrates into the interior of the model. After the water overflowed through the crown of the shaft, the dry area was isolated, which, over time, reduced its volume until the macropore appeared.

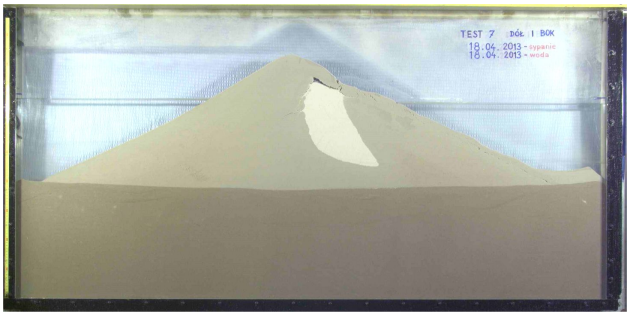

Figure 7: Embankment destruction mechanism (type 2 model) - test with raising the water mirror.

4 Comparison of the physical model and the numerical model

The finite element method has been used to analyse the stability of the flood embankment model, because apart from the value of the stability factor (which is known in advance to be close to one, due to the model-forming method which uses pouring) it usually also provides a realistic process of the destruction mechanism.

In the Plaxis software (version 2; PLAXIS Company, The Netherlands, www.plaxis.nl), it is possible to analyse stability by means of the strength reduction method (the *c-φ reduction* method). This can be done using the Safety module, which enables calculation of the global stability factor, defined as the ratio of the actual value of strength to the reduced value at which generation of the destruction mechanism takes place. The output strength parameters of soil – the angle of internal friction φ and cohesion c – are proportionally reduced during calculations, according to the correlation (1) which thereby defines the value of the stability factor:

$$\sum M_{sf} = \frac{\tan\phi_w}{\tan\phi_z} = \frac{c_w}{c_z} \tag{1}$$

Indices: F – stability factor, M_{sf} – reduction factor, "w" – means the output value, "z" – the reduced value.

One advantage of using the Safety module is not only the ability to determine the value of the embankment stability factor, but also the ability to automatically obtain a sequence corresponding to that factor in the destruction mechanism (there is no need to assume this mechanism as, for instance, in the Bishop method). This results in the ability to compare the factual experimentally determined destruction mechanism to the calculated one, and thereby the ability to verify the quality of the numerical simulation using the finite element method.

Two model geometries have been analysed – type 1 (Figure 8) and type 2 (Figure 9) [3].

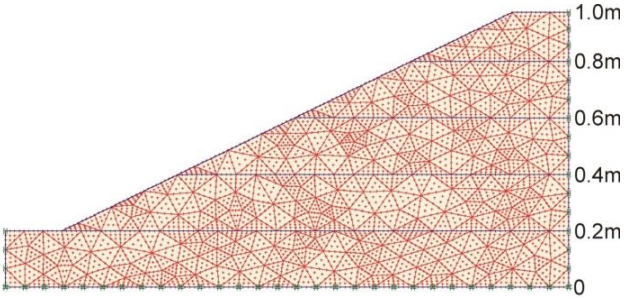

Figure 8: Geometric model of the slope (type 1 model) of a flood embankment designed in the Plaxis software.

The values of material parameters for both types of sand are listed in Table 2. Because only the stability of the models was examined, the same values of stress-strain parameters (ν and E) were adopted for both sands (the stress-strain parameters do not affect the results of the stability analysis using the strength reduction method). The calculated values of the angles of internal friction of soils were adopted based on the experimentally calculated angles of natural slope. The value obtained in this manner for the Lubiatowo sand was lower by several degrees than the one

Table 2: Calculation parameters for the Lubiatowo sand and fine quartz sand.

ID	Name	γ_d [kN/m^3]	ν [-]	E [kN/m^2]	c [kN/m^2]	φ [°]
1	Lubiatowo sand	17.0	0.3	50000	0.1	26
2	fine quartz sand	15.6	0.3	50000	0.1	34

γ_d - bulk density of dry soil, ν - Poisson's ratio, **E** – elastic modulus, **c** – soil cohesion, φ - internal friction angle of soil.

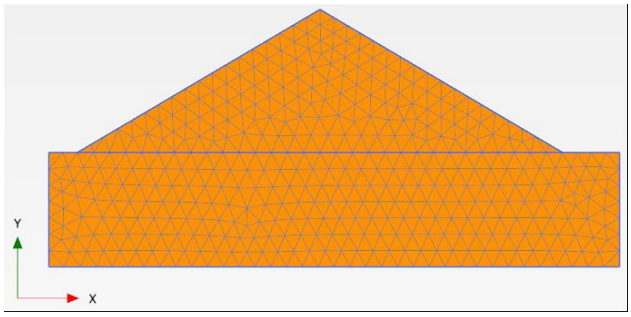

Figure 9: Geometric model of a complete flood embankment model (type 2 model) designed in the Plaxis software.

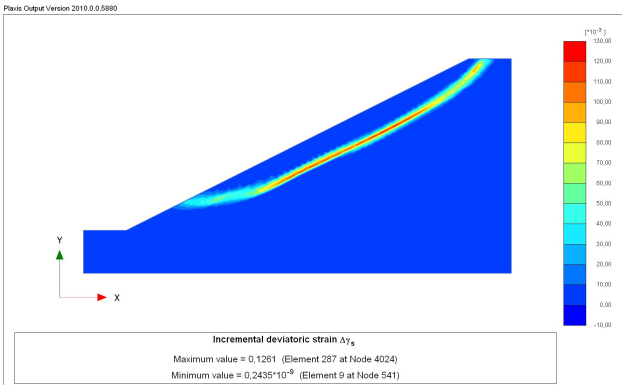

Figure 10: Theoretical embankment destruction mechanism of a flood embankment model, corresponding to the value of the stability factor F = 1.09.

acquired in the triaxial shear test apparatus for a medium dense sample. The minimum value of cohesion (0.1 kPa) associated with the initial soil humidity was adopted for the calculations.

5 Results and discussion

As a result of the conducted calculations, the initial value of the stability factor was obtained for the tests: F = 1.09, as expected (the safety margin for the embankment being very small). The destruction mechanism corresponding to this value is presented in Figure 10, which constitutes a map of increments of the shear modulus. At a point close to the loss of stability, one can observe the location of said increments in the numerical model, and thus a spontaneously generated slide plane of the slope. The lighter the color determines the theoretical mechanism of destruction, the red color means areas with high risk of destruction model.

The path of the slide plane in Figure 10 is typical of cohesionless soils, and in its central part it exhibits the nature of a flat slide. The boundary conditions imposed by the inflexible frames of the rig result in the curvature of this plane in its upper and lower parts. The lower segment intersects the line of the slope at a height of approximately 20 cm.

Superimposing a sample factual embankment destruction process recorded during test F9 in Figure 10, the result image is presented in Figure 11.

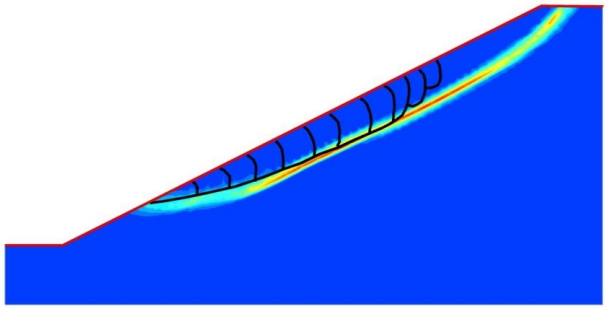

Figure 11: The factual destruction mechanism in the form of a series of micro-slides observed during test F10, superimposed over a theoretical destruction mechanism obtained using the strength reduction method.

The factual destruction mechanism progressed from the bottom. Figure 11 shows that the recorded micro-slides advanced along the surface, which in approximately two thirds of its length, as measured from the bottom, corresponds very well to the theoretical slide plane.

An analogical analysis conducted for the geometry presented in Figure 9 (test type 2) resulted in a stability fac-

tor value of F = 1.07, which indicates the proper selection of the material parameters of the soil. The destruction mechanism corresponding to this value, visible on the map of increments of the shear modulus, is presented in Figure 12. It involves flat slides beginning at the top of the model, as observed in reality (no series of micro-slides has been observed).

The geometric relationship between the destruction mechanism and a single open macropore during the test on the type 2 model is shown in Figure 13, where the red line marks an outline of a macropore – as seen, its upper edge is tangent to the slide plane determined theoretically.

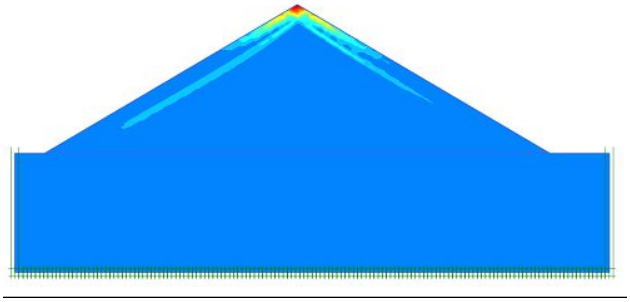

Figure 12: Theoretical destruction mechanism of a complete flood embankment model, corresponding to the value of the stability factor F = 1.07.

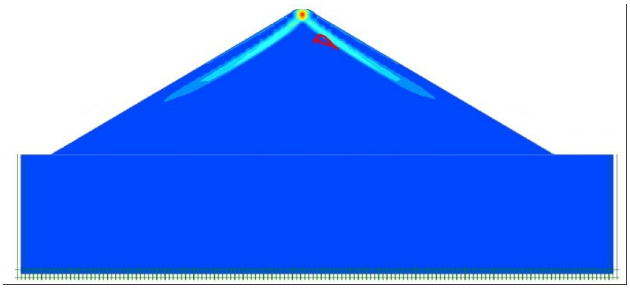

Figure 13: An outline of a macropore from test of model type 2, superimposed over a theoretical destruction mechanism, obtained using the strength reduction method.

Based on an analysis using the Plaxis 2D software for the type 1 model, it can be concluded that the observed micro-slides do not constitute the fundamental destruction mechanism, which involves the movement of an elongated lump, separated by the slide line and corresponding in shape to the area between the slide plane and the slope line in Figure 9. The lack of continuous movement of this lump, as well as its splitting into smaller parts, detached from the whole in the form of micro-slides, are probably associated with the sand gaining a certain false cohesiveness during saturation of the model, related to the increase in humidity.

The geometric relationship between the destruction mechanism and a single open macropore during the test on a complete model (type 2 model) is shown in Figure 13, where the red line marks an outline of a macropore – as seen, its upper edge is tangent to the slide plane determined theoretically.

If we link the location of macropores in selected tests to the mechanism of advancing destruction by means of the micro-slide method, it can be concluded that they can contribute to the destruction of the flood embankment construction.

6 Conclusions

As a result of the study, it was found that the macropores opening mechanism, preceded by the formation of a feed area in which air is cut off from contact with the atmosphere, to the best knowledge of the authors, has not been described in the literature to date. Its exact description requires further research, but based on the conceptual model proposed in the work, it is possible to qualitatively explain the processes leading to such open discontinuities in the soil. The formation of open discontinuities in the body of the flood embankment undoubtedly has a negative impact on its strength - we can imagine that if groundwater continuity is lost in laboratory conditions where the shaft model is built of homogeneous material, the easier it can be to reach that kind of phenomena in real conditions when the shaft creates a random mix of different land. Macropores opening during irrigation of the initially dry shaft model was found for all irrigation scenarios (rain simulation, water level rise on the shaft end, overflow), except for slowly raising water levels and low flow. However, during the simulation of intense rainfall and overflow with sufficient expenditure, the highest number of macropores occurred.

The geometric relationship between the destruction mechanism and a single open macropore during the test on a complete model (type 2 model) is shown in Figure 13, where the red line marks an outline of a macropore – as seen, its upper edge is tangent to the slide plane determined theoretically.

The location of the macropores depends on the watering pattern, as shown in Figure 4, which shows the position of the largest observed macropores in the flood divider

model. Visible, is the local statistical spread of macropore locations, however, they focus, regardless of how the model is watered, at half its height (0.5m). This is a hard to explain regularity, suggesting, however, that the opening of the macropore does not depend on the level of stress in the model.

References

[1] Abo Elela M. M. I. 1996. Filtration phenomena in earth dike during intensive precipitation. PhD Thesis, Polish Academy of Sciences, Institute of Hydro-Engineering, Gdansk

[2] Bogacz, P., Kaczmarek J., Leśniewska D. 2008. Influence of air entrappment on flood embankment failure mechanism – model tests. Technical Sciences, No. 11, Y 2008, 188-201.

[3] Bogacz, P. 2013. Problems of degradation of flood embankments under variable irrigation conditions. PhD Thesis, University of Technology, Koszalin

[4] Kaczmarek J., Leśniewska D. 2010. A flood embankment under changing water level conditions – a comparison of physical and numerical model. Technical Sciences, No. 13, Y 2010, 53-63.

[5] Fredlund D. G., Rahardjo H. 1993. Soil mechanics of unsaturated soil, John Willey and Sons, New York, 1993

[6] Kaczmarek J., Leśniewska D. 2011. Modelling events occurring in the core of a flood bank and water initiated by changes in the groundwater level, including the effect of seepage. Technical Sciences, No. 14(2), Y 2011, 143-152.

[7] Kolbuszewski I. J., Jones R. H. 1961. The preparation of sand samples for laboratory testing, Proc. Hidland Soil Mechanics and Foundation Engineering

[8] Leśniewska D., Bogacz P., Kaczmarek J. & Zaradny H. 2008. Air trapping phenomenon and cracking. Model tests on flood embankment. Floodsite Project report: www.floodsite.net

[9] Leśniewska D., Zaradny H., Bogacz P., Kaczmarek J. 2008. Study of flood embankment behaviour induced by air entrapment. in: Flood risk management: research and practice, Red. Paul Samuels, Stephen Huntington, William Allsop, Jackie Harrop, London: Taylor and Francis Group, s. 655-665

[10] Shin H., Santamarina J. C., 2011. Open-mode discontinues in soils, Geotechnique Letters 1

[11] Sills G. C., Wheeler S. J., Thomas S. D., Gardner T. N. 1991. Behaviour of offshore sols containing gas bubbles, Geotechnique 41, No. 2, 1991

[12] Wheeler S. J. 1986. The stress-strain behaviour of soils containing gas bubbles, The Degree of Doctor of Philosophy, The University of Oxford, Hilary 1986.

[13] Wheeler S. J. 1988. The undrained shear strength of soils containing large gas bubbles, Geotechnique 38, No. 3, 1988

[14] Wichman B. G. H. M., Greeuw G. 1997. Effect of biogenic gas on consolidation parameters of sludge. Proceedings of International Conference on Contaminated Sediments at Rotterdam, 1997

[15] Vaughan P. R. 2003. Observations of the behaviour of clay fill containing occluded air bubbles, Geotechnique 53, No.2

[16] Zaradny H. 1992. Experiment setup for simulation of the flow of water and pollutants. Report IBW PAN, 1992, 10 pp., 14 figs.

[17] Zaradny H. 1993. Physical modeling of infiltration into dikes for stability purposes. The second term – 1993, Report IBW PAN, Contract No. DWW-510, 1993, 24 pp.

[18] Zaradny H. 1994. Physical modelling of infiltration into dikes for stability purposes. The final report., Report IBW PAN, Contract No. DWW-510, 1994, 29 pp.

Sciences Grants: FLOODsite Integrated Project (*Integrated Flood Risk Analysis and Management Methodologies)*, 2004-2009, EU Framework Programme VI, coordinator: HR Wallingford, Great Britain, contract no. GOCE-CT-2004-505420.

TROIAnet network - Ministry of Science (Ministerstwo Nauki), 2009,

Grant of the National Science Centre (Narodowe Centrum Nauki), no. NN 506 31 70 39 "Study of microstructural changes in soil and its effect on the processes of water flow and transport of contaminants in flood embankments" (2010-2013).